JOURNAL OF MATERIALS SCIENCE **36** (2001) 3909–3917

Fine-tuning of temperature coefficients of capacitance (TCC) and dielectric constant (TCK) of Mg_2SnO_4 via second phase addition

A.-M. AZAD*
Advanced Materials Research Center, SIRIM Berhad, P O Box 7035, 40911 Shah Alam, Selangor, Malaysia
E-mail: azad@nextechmaterials.com

Fine-tuning of the temperature coefficients of capacitance and dielectric constant of magnesium orthostannate (Mg_2SnO_4) has been attempted by means of Sn (IV) and Zr (IV) oxide incorporation as a second phase. The additives were also employed to enhance the density and minimize or eliminate porosity at lower sintering temperatures. Phase-pure magnesium stannate powder was synthesized via conventional solid-state reaction. It was mixed with ZrO_2 and/or SnO_2 and sintered in the temperature range 1500°–1600°C for up to 6 h. Electrical measurements using an AC immittance spectroscopic technique over the temperature range 25°–300 °C, on Mg_2SnO_4 compacts containing 5 wt.% of additives and sintered at 1500 °C/ 6 h, were carried out. Data analyses revealed that the capacitance and the derived dielectric constant remained invariant over more than 3 decades of frequency in the kilo to megahertz regime. It was also found that addition of ZrO_2 and SnO_2 has a benign effect on both temperature coefficient of capacitance (TCC) and temperature coefficient of dielectric constant (TCK) as it resulted in smaller dependence of capacitance and dielectric constant compared to pure Mg_2SnO_4. Typically, the TCC values were 5 and 30 ppm/°C and TCK values were 20 and 30 ppm/°C for 5 wt.% ZrO_2- and 5 wt.% SnO_2- added Mg_2SnO_4, respectively, in the temperature range 25°–300 °C.

1. Introduction

The alkaline-earth stannates having the general chemical formula $MSnO_3$ (M = Ca, Sr and Ba), have recently been studied as potential electronic ceramics, such as thermally stable capacitors with low permittivity and small loss tangent [1–5] finding applications such as a dielectric plate in ceramic filters for cellular phones and in high speed computing devices. Pure, as well as the doped varieties of these stannates are also being targetted for use as air-to-fuel (A/F) ratio sensors in automobiles. Interestingly, even though magnesium is a member of the alkaline-earth metal group to which Ca, Sr and Ba belong, no reliable technical information on the electrical behavior of the compounds in the pseudobinary MgO-SnO_2 system appears to exist in the published literature. A limited amount of literature is available on the synthesis aspects of compounds in Mg-Sn-O system. Only the pressure-temperature relationship has been reported in the literature; no reliable composition-temperature phase diagram exists [6]. On the other hand, corresponding titanates ($MgTiO_3$, Mg_2TiO_4 and $MgTi_2O_5$) and silicates ($MgSiO_3$, steatite and Mg_2SiO_4, forsterite) are commercially produced as low dielectric constant, high resistance and low TCK (temperature coefficient of dielectric constant) components [7]. In addition, the behavior of magnesium metastannate ($MgSnO_3$) and orthostannate (Mg_2SnO_4) is totally different from the corresponding Ca, Sr and Ba counterparts. The meta- and orthostannates of calcium, strontium and barium are known to be stable independently up to very high temperatures without disproportionation. $MgSnO_3$ is unstable and disproportionates into orthostannate and tin oxide upon heating above ~700 °C. In some cases, even the orthostannate cannot be synthesized as a single-phase [8]. No correlation has been established among important parameters, such as, synthesis, processing, microstructure and electrical behavior of these materials; such a correlation is necessary to understand the underlying mechanisms in the electrical components made from the materials.

In view of the information gaps in the reported research and lack of data on the electrical properties envisaged in magnesium stannates, akin to those in the corresponding silicates and titanates, systematic investigations were carried out in MgO-SnO_2 system and have recently been reported elsewhere [9–10]. It was found that magnesium orthostannate could be sintered into dense bodies with near zero porosity upon soaking for 2 h at 1600 °C. Electrical measurements carried out on dense compacts of Mg_2SnO_4 revealed that this is

Present Address: NexTech Materials Ltd., 720-I Lakeview Plaza Blvd., Worthington, OH 43085, USA.

a high resistance, low capacitance, low dielectric constant and low loss material. In addition, the capacitance and the dielectric constant showed very small variation with temperature in the range 25°–300°C over a wide frequency domain. In order to achieve density enhancement and porosity minimization/ elimination and to modify the electrical behavior of parent stannate, two different additives, viz., ZrO_2 and SnO_2 were employed. The results of such a study on the effect of foreign additives are discussed in this paper.

2. Experimental

2.1. Sample preparation and characterization

SnO_2 (99.995% powder) and ZrO_2 (99.99% powder) from Aldrich (Milwaukee, USA) and MgO (99% powder) and $Mg(NO_3)_2{\cdot}6H_2O$ (99% deliquescent crystals) from BDH (Poole, UK), were used as the starting materials. The samples investigated in this work were synthesized via the traditional solid-state reaction (SSR) route. A detailed description of the technique for the synthesis of pure Mg_2SnO_4 has been reported elsewhere [9]. However, a brief account of the same as well as that for the synthesis of 2-phase mixtures with ZrO_2 and SnO_2 is given here.

The stoichiometric quantities (2:1 molar ratio) of MgO or $Mg(NO_3)_2 \cdot 6H_2O$ and SnO_2 powder of stated purity were accurately weighed (to give about 100 g of the final product after calcination) and dry mixed in an agate mortar. The mixture was then ball-milled for 4 h in airtight polystyrene bottles using acetone as a liquid medium and clean zirconia balls as the milling media. The slurry was dried first at room temperature in a ventilated fume hood and then in an air oven. The dried mass was crushed and pulverized in an agate mortar and pestle to fine powder and calcined first at 800 °C for 8 h then at 1200 °C for 12 h. After the calcination step, the powder was subjected to phase analysis using powder X-ray diffraction at room temperature using Cu K_α radiation ($\lambda = 1.5406$ Å) in the 10°–80° (2-θ) range to confirm the formation of the targeted compound as a single phase. The resulting X-ray diffraction (XRD) pattern was also used to detect the presence of, if any, unreacted starting materials and/or other phases. In some cases, XRD was also performed on sintered discs and powders in order to confirm that the chemical composition remained unaltered.

The calcined powder was subjected to sintering at 1500 and 1600 °C, for soak times ranging from 2 to 6 h in ambient air. Prior to sintering, the calcined powder was blended with polyvinyl alcohol (aqueous solution containing 40 gl^{-1} PVA) as a binder, dried overnight and pressed into discs of 12 or 15 mm diameter and 2–3 mm thick by uniaxial compaction at pressures not exceeding 40 MPa. In the case of 2-phase compositions, 5 wt.% ZrO_2 and SnO_2 were used. For the sake of ease in identification, these samples will be subsequently referred to as MS (pure Mg_2SnO_4), MSZ5 (for zirconia doped) and MST5 (for tin oxide doped). Each composition (25 g batch) was obtained by thoroughly mixing appropriate amounts of Mg_2SnO_4 powder with ZrO_2 or SnO_2, ball milling, adding binder and sintering in different schedules as outlined in Table I.

TABLE I Sintering schedules for the various systems studied in this work

Sample designation	Composition (wt.%)	Sintering schedule
MS	Mg_2SnO_4	1500 °C/ 6 h; 1600 °C/2 h
MSZX	$Mg_2SnO_4 + 5\ ZrO_2$	1500 °C/ 6 h
MSTY	$Mg_2SnO_4 + 5\ SnO_2$	1500 °C/ 6 h

A Horiba (CAPA-700 model, Japan) particle size analyzer was used to estimate the particle size and its distribution in the green powders. Densities of the sintered samples were measured both by: (a) pycnometry (He gas AccuPyc 1330, Micromeritics, USA) and, (b) Archimedes principle of water displacement. The ratio of (b) to (a) was used to indicate the fractional theoretical density achieved in the samples at a given temperature and time of sintering. Microstructural features of the starting green powders as well as the sintered discs were determined by using a JEOL-6400SM scanning electron microscope. Semi-quantitative compositional analyses in different region of the sintered samples were carried out by energy dispersive analysis by X-rays (EDX) on a system attached to a Philips XL40 scanning electron microscope. The sintered sample specimen were fractured and mounted on aluminum stubs, without polishing or etching. Micrographs were also collected on as-sintered surfaces to discern non-uniformity, if any, of grain growth, intergranular connectivity and porosity in the bulk and the surface.

2.2. Electrical measurements

Electrical measurements were carried out on sintered specimens over a wide range of applied frequencies ($5\ \text{Hz} < f \leq 13\ \text{MHz}$) using a HP4192A LF Impedance Analyzer (Hewlett-Packard, Yokogawa, Japan) between room temperature and 300 °C. The data acquisition was accomplished using fully automated experimental control via a desktop personal computer.

A special in-house designed and fabricated all-stainless-steel sample holder was used. The holder was fitted with square blocks via adjustable screws on both sides. Gold wires, 0.25 mm in diameter (99.99% pure, Goodfellow, Cambridge, UK) welded to freshly cut circular gold foils (99.95% pure) from the same supplier, were used as electrode leads. The sintered disks were snugly sandwiched between the gold foils. This subassembly (of the sample and the electrode combination) was inserted between two clean 20 mm square high purity high density alumina plates, which were then clamped tightly between the steel blocks on the holder. Each sample was introduced into the uniform temperature zone of a custom-designed small, low-thermal mass, precalibrated box furnace. The furnace was slowly heated to the desired temperature, at a rate of less than 1°C min^{-1}. Sufficient time was allowed to equilibrate at the measurement temperature within the sample before the acquisition of ac electrical

data. The temperature fluctuations at the measurement points were not more than ±0.5 °C. The normal waiting time at each measurement temperature was about 15–30 minutes, after the desired temperature was reached. After this, about 90 minutes were given to acquire electrical data over the entire frequency range. This facilitated the data acquisition on the same sample at an isothermal dwell for many times. The sample thickness and the electrode area in all the measurements were kept as much constant as possible so that the geometric configuration produced a fixed effect on the terminal immittance data. Thus, the terminal immittance data did not require normalization.

In order to examine the reversibility of the electrical behavior of a given sample, electrical measurements were carried out during the heating and the cooling mode, allowing more time for thermal equilibration and data acquisition during cooling for obvious reasons. In all the cases, samples were also held at elevated temperatures overnight to detect any deviation in the electrical characteristics during such longer soak-times. Generally, each sample was made to undergo several thermal cycling between room temperature and 300 °C over a period of 7–12 days. This also constituted what is known as an *accelerated test* as employed in electronic industries on electronic components to assess their shelf life and rate of failure under extreme conditions.

Measurement of breakdown voltage was also carried out. For this purpose a voltage breakdown instrument (CEAST model 6135, Italy) was used. The samples were clamped between two metallic electrodes in a dry air chamber. These were subjected to an applied voltage at a rate of 500 Vs^{-1} in a continuous sweep mode. From the breakdown voltage and the thickness of the samples, the dielectric strength was computed.

3. Results and discussion

3.1. Structural and microstructural artifacts in the sintered bodies

Particle size analysis of the pure magnesium orthostannate powder obtained after calcination at 1200 °C/12 h showed that 50% of the particles were less than 1 μm in size while 35% were within the range 1–2 μm. Similar analysis of the as-received commercial SnO_2 and ZrO_2 powders used in this study revealed that about 78 and 91% of the particles were of submicron size in the two cases, respectively. The XRD signatures of MS, MST5 and MSZ5, sintered at 1500 °C for 6 h are compared in Fig. 1. It can readily be seen that the principal phase in all the three cases is Mg_2SnO_4; only 1 additional peak (marked as *) in the diffractograms of MSZ5 and MST5 could be observed, beside an unknown diffraction peak at 2-$\theta \sim 78.6°$. Thus, it can be inferred that addition of 5 wt.% of either of the two oxides, did not cause any phase change. Absence of the expected characteristic peaks belonging either to ZrO_2 or SnO_2 within the detection limits of X-ray technique, could be due to the small amount of the additives employed. No experimental data with respect to the solid solubility of ZrO_2 or SnO_2 in Mg_2SnO_4 is available in the literature to suggest or negate the speculation that the two oxides might form a solid solution in the inverse spinel stannate.

In order to highlight the salient microstructural features of the sintered MSZ and MST samples, it is worthwhile to consider microstructural evolution in pure magnesium orthostannate as well. This is shown for typical MS samples soaked for 6 h at 1500 °C and 2 h at 1600 °C, in Fig. 2. These micrographs illustrate the densification and increase in intergranular contact as a function of sintering time and temperature. While near perfect densification (with almost zero porosity) in samples sintered at 1600 °C/2 h can be clearly seen, pores

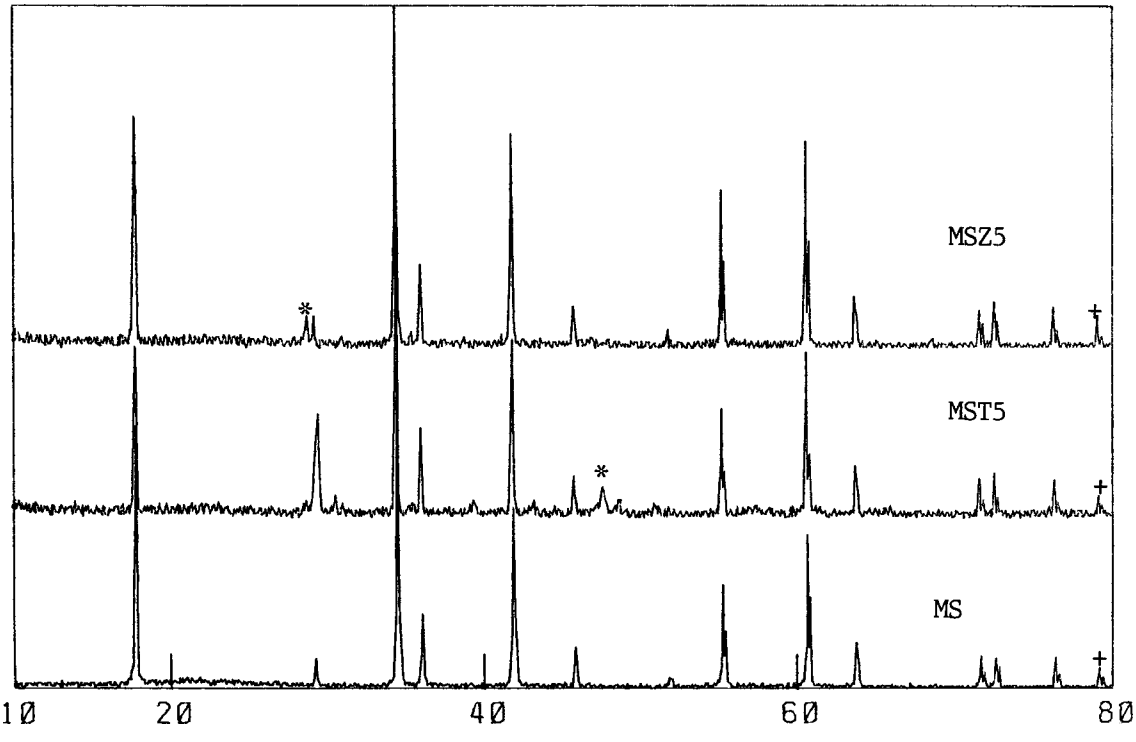

Figure 1 Comparative XRD signatures of MSZ5, MST5 and MS sintered pellet at 1500 °C/6 h. (+: unknown peak).

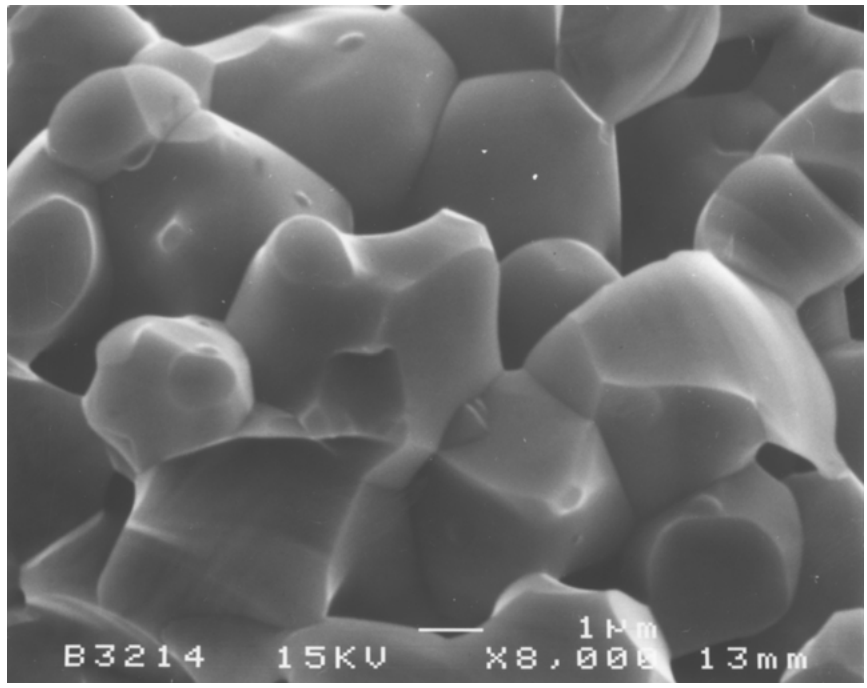

(a)

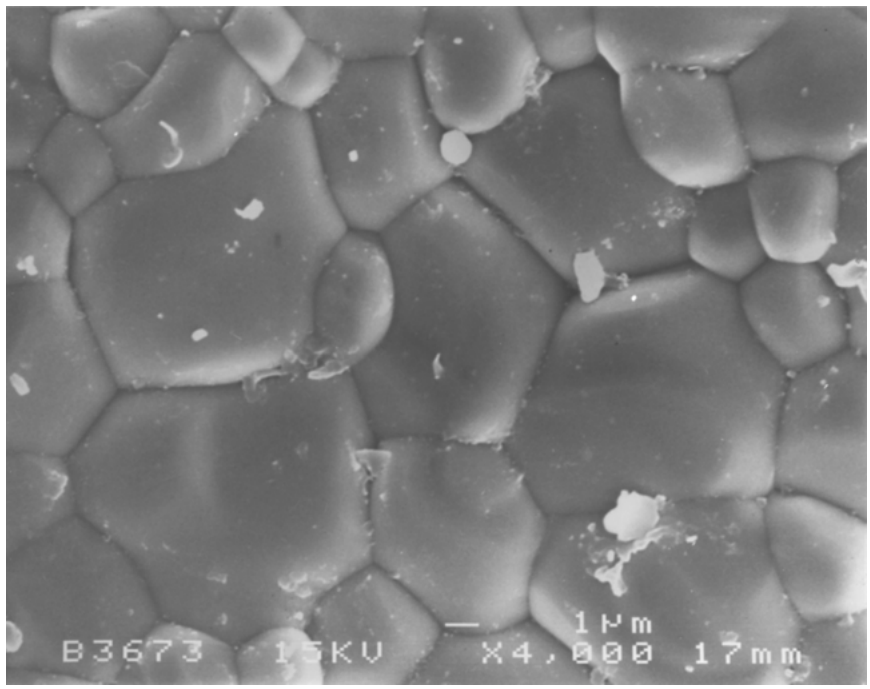

(b)

Figure 2 Microstructural artifacts of MS samples sintered at: (a) 1500 °C/6 h and (b) 1600 °C/2 h.

could not be eliminated effectively in the compacts sintered at 1500 °C. Nevertheless, the remnant porosity in the bodies sintered at 1500 °C is isolated in nature and in fact, did not impart any noticeable detrimental effect on the electrical characteristic of the material [11]. The theoretical weight ratio of tin-to-magnesium $[(Sn/Mg)_{w/w}]$ in Mg_2SnO_4 is 2.44. EDX analysis, using the standardless ZAF quantification method on several randomly chosen grains and at the grain boundaries of sintered MS samples, yielded a tin-to-magnesium weight ratio of 2.423, thereby showing the average grain composition to be pure Mg_2SnO_4. However, individually, the grain boundaries were slightly depleted in tin, while the grains were richer in tin. This could be attributed to the material loss via surface evaporation of SnO_2 from the grain boundaries and disproportionation at high temperatures according to the reaction:

$$SnO_2\ (s) \rightarrow SnO\ (g) + 1/2\,O_2$$

This would upset the concentration equilibrium thereby making the grains appear slightly rich in tin relative to the grain boundaries.

The microstructural features of the as-sintered and fractured surfaces of MSZ5 bodies soaked at 1500 °C for 6 h are shown in Fig. 3. The surface (Fig. 3a) shows a highly porous structure, with two distinct morphologies. The magnesium orthostannate grains are seen interconnected via tetragonal zirconia polycrystals. However, the microstructure of the fractured surface shows

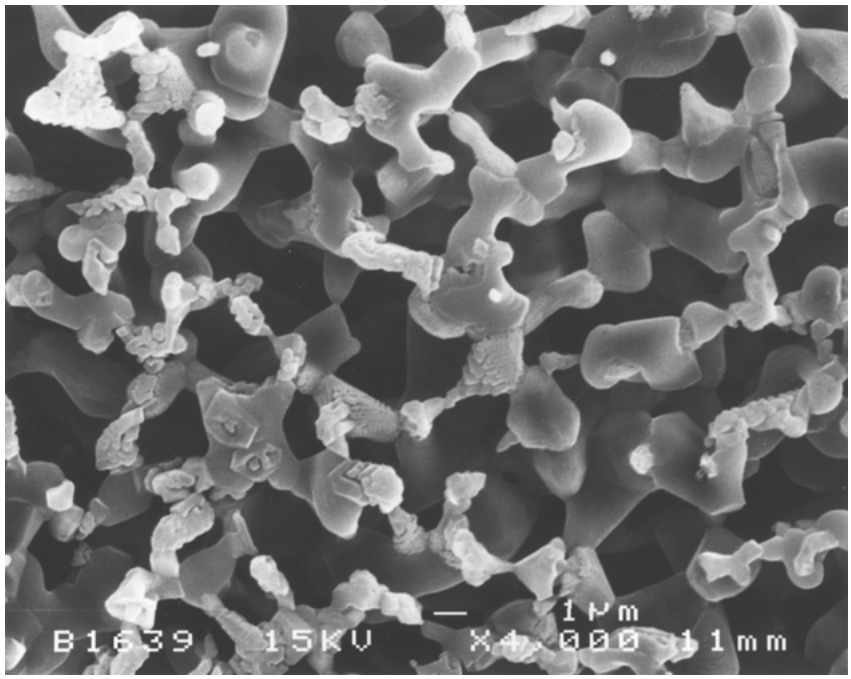

(a)

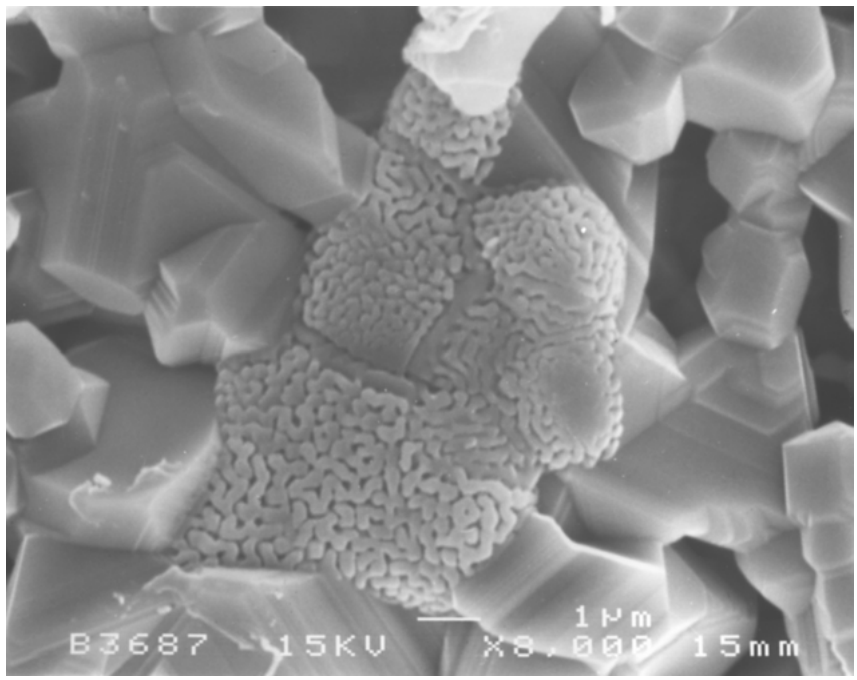

(b)

Figure 3 Microstructural development in MSZ5 compacts soaked for 6 h at 1500 °C: (a) Mg_2SnO_4 skeletons interconnected via polycrystalline tetragonal zirconia shoulders and (b) fractured surface revealing segregated lacy zirconia network.

a relatively dense body with a significant degree of intergranular connectivity. The segregation of zirconia in pockets surrounded by the stannate grains, nevertheless, is an interesting artifact of MSZ5 samples. A typical EDX point analysis on the MSZ5 sample is shown in Fig. 4. The semi-quantitative analysis of a grain in the lacy region yielded a value of 75.64 for the weight percent of Zr, in addition to small concentrations of Sn and Mg, which is in excellent agreement with the theoretical value of 74.03% for Zr in pure ZrO_2 (uncertainty of the measurements by EDX $\sim \pm 3\%$). Thus, these are indeed ZrO_2 grains.

The microstructural feature surface of MST5 soaked at 1500 °C for 6 h is shown in Fig. 5; enhanced grain growth and reduced porosity is evident from this illustration.

3.2. Electrical response

The acquired AC electrical data were in the form of capacitance (C_p) and conductance (G_p) as a function of applied frequency in the range 5 Hz to 13 MHz at temperatures between 25° and 300 °C. From these parameters, the terminal capacitance, dielectric constant (K or relative permittivity, ε_r) and loss tangent ($\tan \delta$) were computed using the following relationships:

$$K \text{ or } \varepsilon_r = C(d/A)/\varepsilon_o \quad \text{and} \quad \tan \delta = G_p/\omega C_p$$

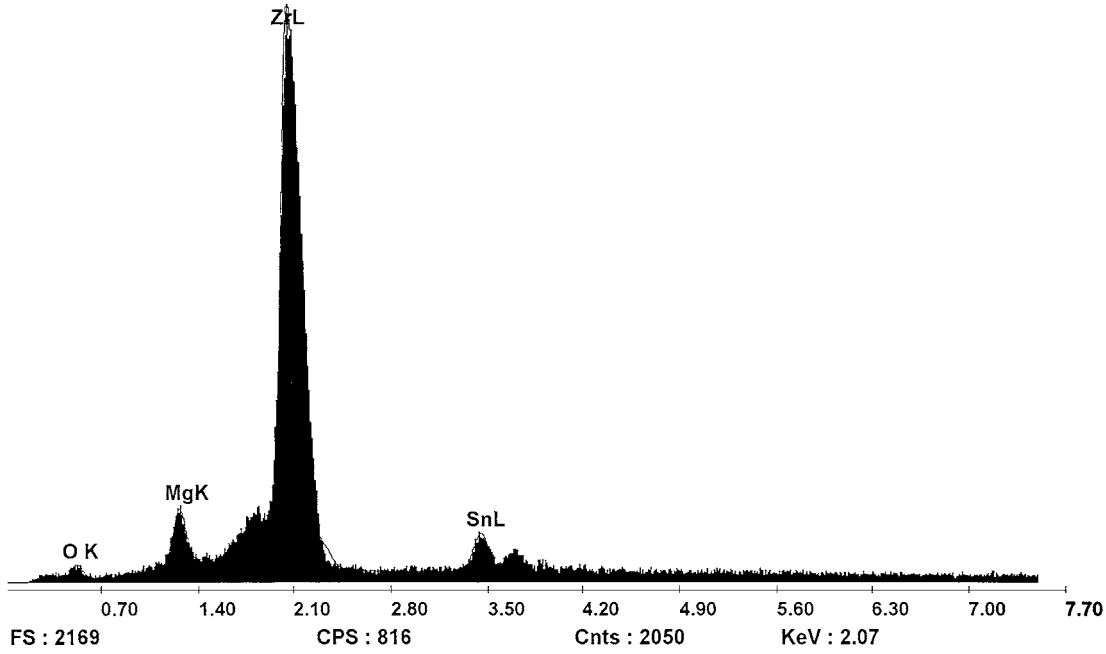

Figure 4 A typical elemental concentration profile by EDAX in the lacy region of MSZ5 sample.

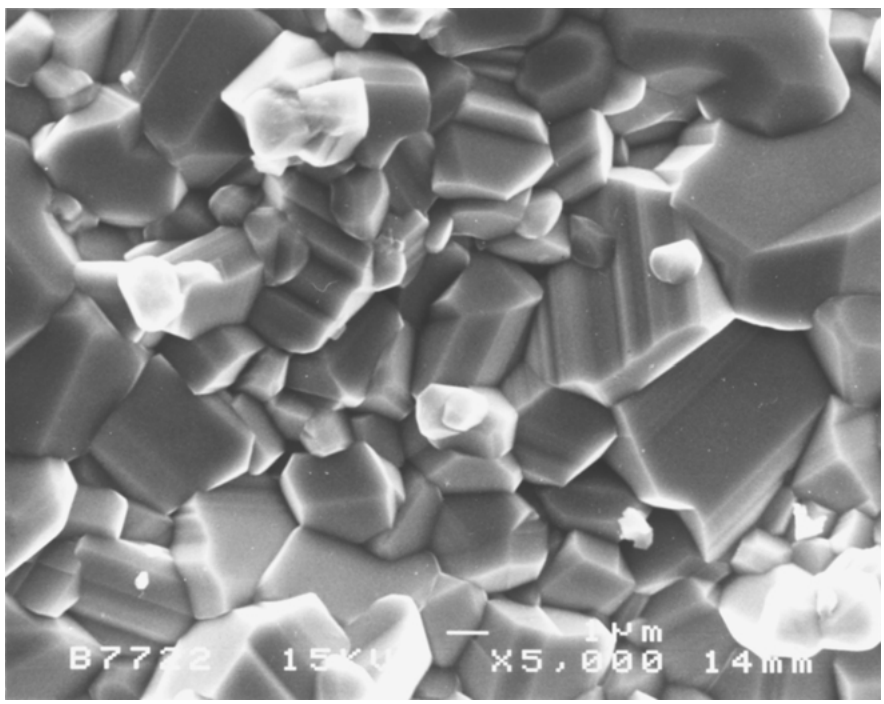

Figure 5 Microstructural artifact of MST5 sample sintered at 1500 °C/6 h.

Where, C = sample capacitance in Farad (F), d = thickness of the sample (distance between the opposite electrodes, m), A = electrode area (m^2), ε_o = permittivity of the vacuum, 8.854×10^{-12} F m^{-1}, ε_r = relative permittivity of the material, and ω = angular frequency = $2\pi f$. The data thus transformed were used to illustrate variation with applied frequency and temperature.

Some typical plots of capacitance (C) and dielectric constant (K) variation with applied frequency in MSZ5 samples sintered at 1500 °C for 6 h, at a few selected temperatures in the range 25°–300 °C are shown in Fig. 6a–d. Several interesting features in these plots can be identified. The data acquired, for example, at any temperature, showed the consistency of frequency dependence of the capacitance values between various runs on a given sample. Such consistency also showed that the furnace temperature during data acquisition was uniform and stable. It further demonstrated that the sample experienced the same temperature during various runs. Furthermore, if there were thermal fluctuations (within the furnace and the sample), they did not necessarily affect the capacitance values appreciably. In addition, the thermal cycling for several times across a given temperature yielded almost identical values of the terminal capacitance over a frequency regime spanning over 3–4 decades. Another interesting feature is that the capacitance and the dielectric constant

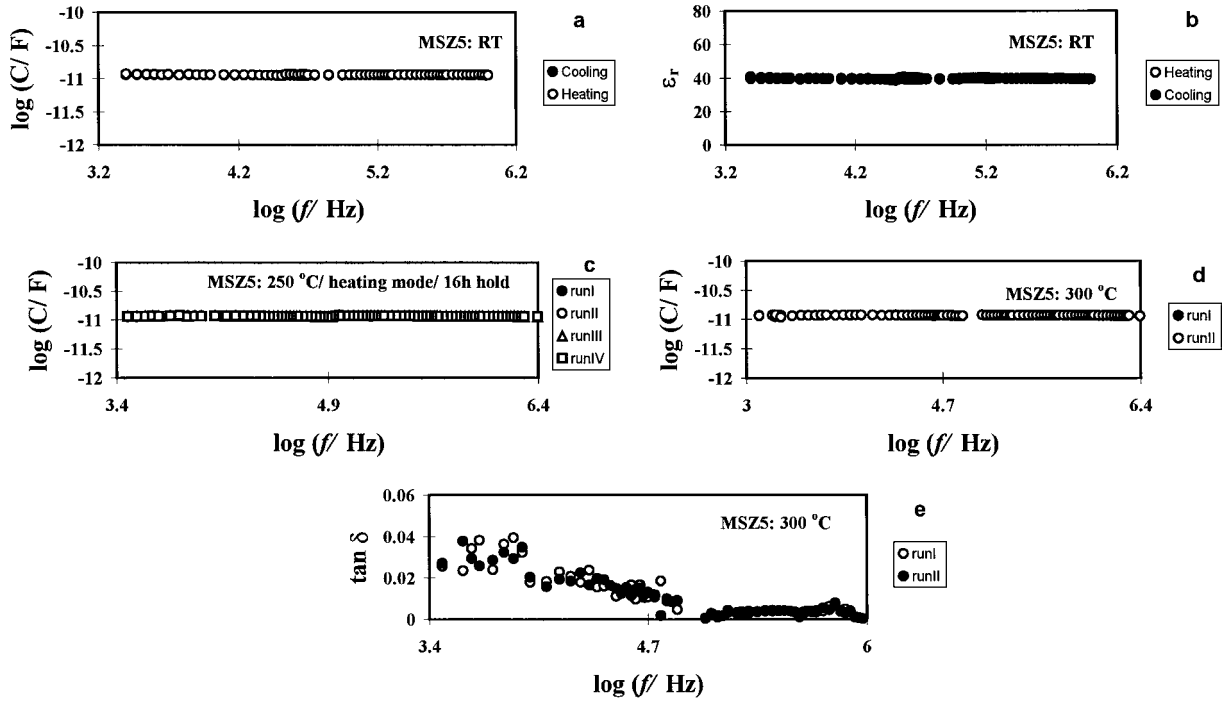

Figure 6 (a–d) Some representative plots showing the consistency of frequency dependence of capacitance and dielectric constant between different runs at different soaking temperatures on randomly selected MSZ5 samples. (e) Variation of loss tangent value with frequency at 300 °C for MSZ5.

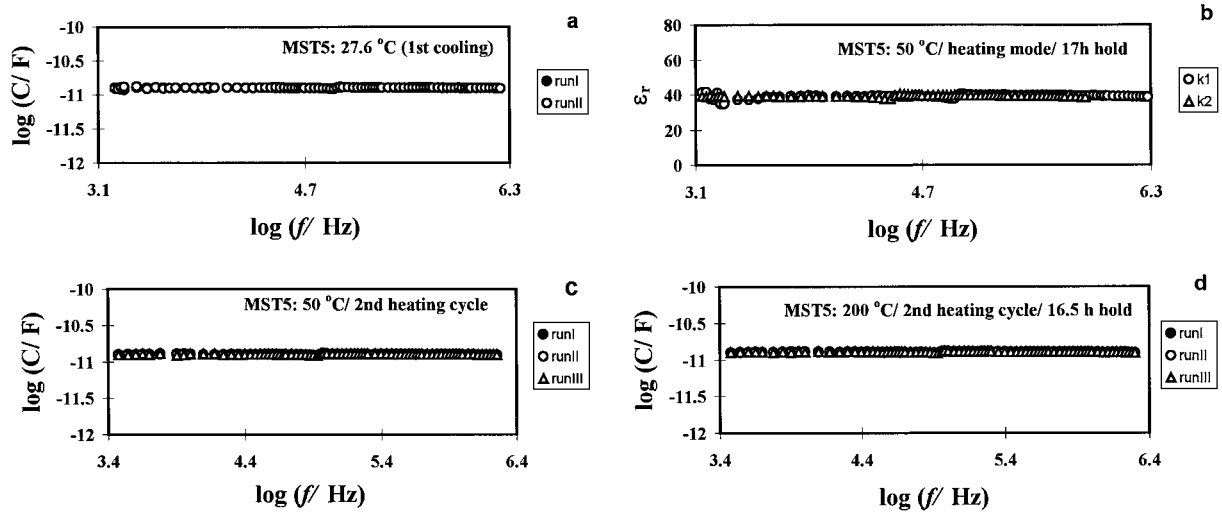

Figure 7 (a–d) Some representative plots showing the consistency of frequency dependence of capacitance and dielectric constant between different runs at different soaking temperatures on randomly selected MST5 samples.

remained almost parallel to the x-(frequency) axis over a wide range, signifying near zero dependence of capacitance and relative permittivity on the applied frequency. This and the fact that no peaks were noticed in the entire frequency domain, shows that the relaxation observed in this material is not a thermally activated process. Finally, the loss tangent shown for illustrative purposes for the sample held at 300 °C (Fig. 6e), is very small over a wide frequency range.

Similar plots of capacitance (C) and dielectric constant (K) variation with applied frequency in MST5 samples sintered at 1500 °C for 6 h, at selected temperatures in the range 25°–300 °C are shown in Fig. 7 a–d. The loss tangent values in MST5 samples held isothermally up to a temperature of 300 °C were also found to be very small and are shown in Fig. 8 for samples heated to 250 ° and 300 °C. The observations made above in the case of MSZ5 samples are equally valid in this case and are identical to those shown by the pure Mg_2SnO_4 samples subjected to similar electrical measurements, albeit with different magnitudes of capacitance and dielectric constant [10, 11].

From the linear portions of the log C vs. log f and ε_r vs. log f plots at different temperatures, average values of capacitance and dielectric constant in the two systems, MSZ5 and MST5, were computed. It was found that the average values of capacitance were 11.2 pF and 12.5 pF while the average ε_r values were 39.1 and 39, for the ZrO_2 and SnO_2-added samples, respectively over the range 27° to 300 °C. In comparison to these, the pure orthostannate was found to possess a capacitance of 18.3 pF and ε_r value of 26.1 [11]; these values

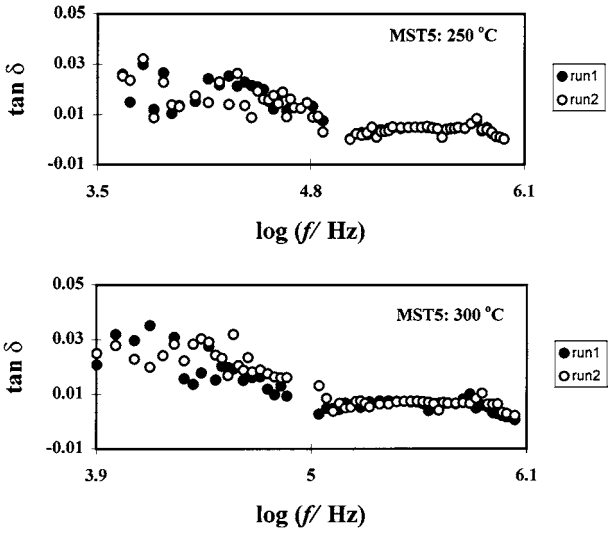

Figure 8 Variation of loss tangent value with frequency for MST5 at 250° and 300 °C.

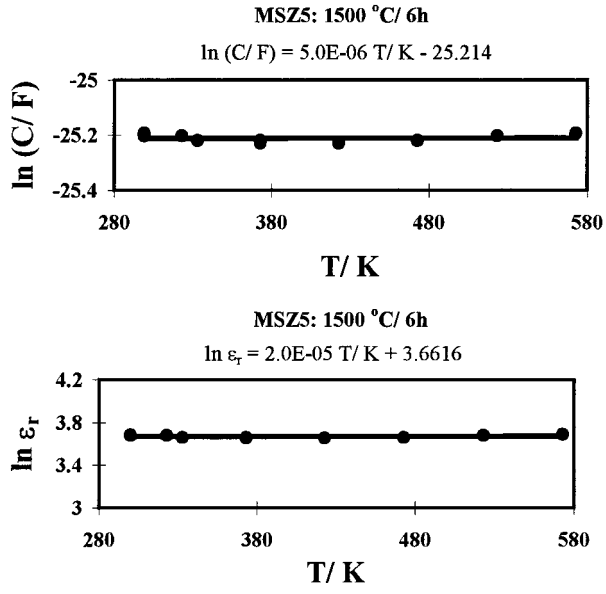

Figure 9 Temperature dependence of capacitance and dielectric constant in MSZ5 samples.

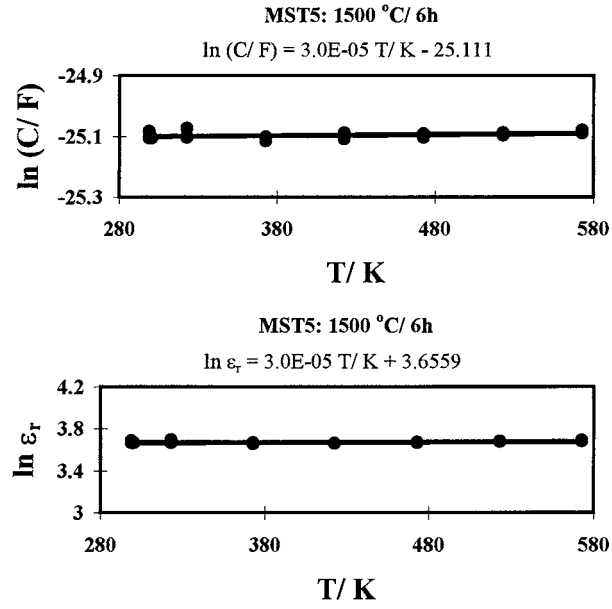

Figure 10 Temperature dependence of capacitance and dielectric constant in MST5 samples.

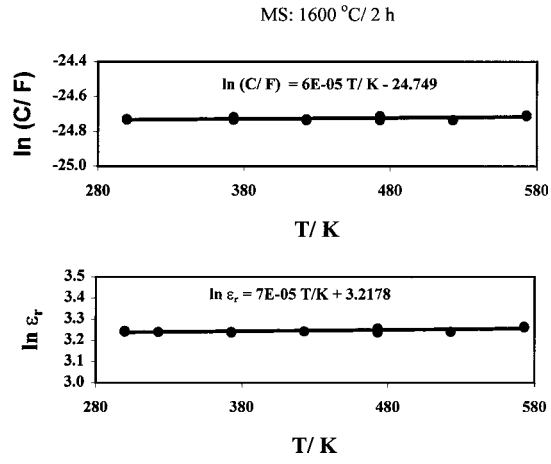

Figure 11 Temperature dependence of capacitance and dielectric constant in MS samples sintered at 1600 °C/2 h.

are somewhat higher (but still small and of the same order) than those previously reported on this system [10] in the same temperature range. These average values plotted against temperature are shown in Figs 9, 10 and 11 for MSZ5, MST5 and MS, respectively. The parametric equations describing the temperature dependence of the two quantities (C and ε_r) obtained from least-squared fitting procedure are also shown on each of the two curves. The near-independence of C and K on temperature is easily manifested in the very small value of the slope of each of the two straight lines. The values of the temperature coefficients of capacitance ($\mathrm{TCC} = 1/C \cdot (\partial C/\partial T)$) and the dielectric constant ($\mathrm{TCK} = 1/K \cdot (\partial K/\partial T)$) were found to be 60 and 70 ppm/°C for MS, 5 and 20 ppm/°C for MSZ5, and 30 and 30 ppm/°C for MST5. Such small coefficients indeed show that the capacitance and the relative permittivity of magnesium stannates (pure and doped) are very weakly dependent on temperature, in the range 25° to 300 °C.

The dielectric strength of the MS, MSZ5 and MST5 samples were found to be 1.66, 1.70 and 1.81 kV, mm^{-1}, respectively, which are not too different from one another.

4. Conclusions

Electrical characteristics of sintered bodies of magnesium orthostannate (Mg_2SnO_4) mixed with 5 wt.% ZrO_2 (MSZ5) and SnO_2 (MST5) were investigated by using an AC immittance technique. Electrical measurements were carried out isothermally at selected temperatures in the range 25°–300 °C over the frequency range of 5 Hz–13 MHz. As a result of this, two novel characteristics were revealed. First, similar to pure Mg_2SnO_4, the capacitance (C) and permittivity (K or ε_r) remained nearly independent of the applied frequency in MSZ5 and MST5 samples, at each of the 7 temperatures at which electrical measurements were carried out. Second, these two parameters showed extraordinarily weak dependence of temperature. In addition, the values of

TCC and TCK in the MSZ5 and MST5 are close to each other, being not very different from those in pure Mg_2SnO_4. It is thus possible to tailor the TCC and TCK values of this ceramic system by appropriate material incorporation and suitable processing to meet the requirements of a given application.

References

1. A.-M. AZAD and N. C. HON, *J. Alloys Comp.* **250** (1998) 95.
2. A.-M. AZAD, L. L. W. SHYAN and P. T. YEN, *ibid.* **282** (1999) 109.
3. A.-M. AZAD, L. L. W. SHYAN, P. T. YEN and N. C. HON, *Ceram. Int.* **26** (2000) 685.
4. A.-M. AZAD, L. L. W. SHYAN and M. A. ALIM, *J. Mater. Sci.* **34** (1999) 1175.
5. *Idem.*, *ibid.* **34** (1999) 3375.
6. A. E. RINGWOOD, *Earth Planet. Sci. Lett.* **5** (1968) 245.
7. J. M. HERBERT, "Ceramic Dielectrics and Capacitors" (Gordon and Breach Science Publishers, Philadelphia, 1985).
8. G. PFAFF, *Thermochim. Acta* **237** (1994) 83.
9. A.-M. AZAD and L. J. MIN, *Ceram. Int.* **27** (2001) 325.
10. A.-M. AZAD, L. J. MIN and M. A. ALIM, *ibid.* **27** (2001) 335.
11. A.-M. AZAD, AMREC Activity Report, December 1999 (unpublished research).

Received 5 July 2000
and accepted 19 March 2001